HHS Public Access

Author manuscript

Genesis. Author manuscript; available in PMC 2021 May 03.

Published in final edited form as:

Genesis. 2020 March ; 58(3-4): e23347. doi:10.1002/dvg.23347.

Drosophila pericentrin-like protein promotes the formation of primordial germ cells

Junnan Fang, **Dorothy A. Lerit**

Department of Cell Biology, Emory University School of Medicine, Atlanta, Georgia

Summary

Primordial germ cells (PGCs) are the precursors to the adult germline stem cells that are set aside early during embryogenesis and specified through the inheritance of the germ plasm, which contains the mRNAs and proteins that function as the germline fate determinants. In *Drosophila melanogaster*, formation of the PGCs requires the microtubule and actin cytoskeletal networks to actively segregate the germ plasm from the soma and physically construct the pole buds (PBs) that protrude from the posterior cortex. Of emerging importance is the central role of centrosomes in the coordination of microtubule dynamics and actin organization to promote PGC development. We previously identified a requirement for the centrosome protein Centrosomin (Cnn) in PGC formation. Cnn interacts directly with Pericentrin-like protein (PLP) to form a centrosome scaffold structure required for pericentriolar material recruitment and organization. In this study, we identify a role for PLP at several discrete steps during PGC development. We find PLP functions in segregating the germ plasm from the soma by regulating microtubule organization and centrosome separation. These activities further contribute to promoting PB protrusion and facilitating the distribution of germ plasm in proliferating PGCs.

Keywords

centrosome; development; germ plasm; primordial germ cell

1 | INTRODUCTION

In many organisms, the germline soma dichotomy is a critical early developmental decision that ensures the proper specification of cellular fate (Benner, Deshpande, & Lerit, 2018). The specification and formation of primordial germ cells (PGCs) is often determined in early embryogenesis through the inheritance of the germ plasm, which contains the maternally derived germline determinants (Ewen-Campen, Schwager, & Extavour, 2010). Segregation of the germ plasm into nascent PGCs represents a key event in germ cell development, as germ plasm is both necessary and sufficient to impart the germline fate (Illmensee & Mahowald, 1974; Lehmann & Nüsslein-Volhard, 1986).

Correspondence: Dorothy A. Lerit, PhD, Department of Cell Biology, Emory University, 615 Michael St., Whitehead Building, Room 444, Atlanta, GA. dlerit@emory.edu.

SUPPORTING INFORMATION

Additional supporting information may be found online in the Supporting Information section at the end of this article.

In *Drosophila melanogaster*, germ plasm assembly occurs during oogenesis and begins with the recruitment of *oskar* mRNA (*osk*) to the posterior pole, reviewed in (Lehmann, 2016; Mahowald, 2001; Williamson & Lehmann, 1996). Translation of Osk protein is facilitated by the RNA helicase Vasa and represents an integral step in germ plasm assembly (Breitwieser, Markussen, Horstmann, & Ephrussi, 1996; Johnstone & Lasko, 2004). Germ plasm localization to the posterior pole is maintained throughout oogenesis and early embryogenesis through its association with the actin cytoskeleton (Forrest & Gavis, 2003; Lantz, Clemens, & Miller, 1999; Sinsimer, Lee, Thiberge, & Gavis, 2013; Vanzo, Oprins, Xanthakis, Ephrussi, & Rabouille, 2007). Because the early embryo develops as a syncytium, the localization and anchorage of the germ plasm facilitates the inheritance of a critical threshold of fate molecules into the presumptive germline and prevents their improper distribution into the soma.

During the first 2 hr of development, the syncytial nuclei undergo repeated rounds of rapid and synchronous divisions coupled to migration prior to the cellularization of the somatic nuclei during nuclear cycle (NC) 14. Nuclear migration and division events are supported by the coordinated activities of the actin cytoskeleton, microtubule network, and centrosomes, which are the microtubule organizing centers of most eukaryotes (Karr & Alberts, 1986; Schejter & Wieschaus, 1993). Coincident with the arrival of several nuclei within the posterior pole region of the embryo, PGCs undergo precocious cellularization during NC 10 (Foe & Alberts, 1983).

PGC formation and the inheritance of germ plasm is also dependent upon the coordination of the cytoskeletal networks. First, physical proximity of the centrosomes to the posterior pole triggers the release of the anchored germ plasm, which actively transits along astral microtubules to coalesce around the centrosomes (Lerit & Gavis, 2011; Raff & Glover, 1989). Second, actin rearrangements at the posterior cortex permit the formation of large membrane protrusions, or pole buds (PBs) (Warn, Smith, & Warn, 1985). Third, the assembly of migrating nuclei, centrosomes, and associated germ plasm is encapsulated within the PB. Finally, PBs cellularize upon the formation of an actin-rich contractile ring that forms at the bud base (Cinalli & Lehmann, 2013; Padash Barmchi, Rogers, & Häcker, 2005; Warn, Smith, & Warn, 1985). Individualized PGCs undergo 0–2 asynchronous cellular divisions prior to gastrulation and gonadogenesis (Mahowald, 2001). Microtubules also facilitate germ plasm partitioning between proliferating PGCs (Lerit & Gavis, 2011).

The association between germ plasm and centrosomes was first demonstrated by ultrastructural studies, which revealed electrondense germ granules in close proximity to the centrioles (Counce, 1963; Mahowald, 1962). Subsequently, in situ hybridization showed the germ plasm mRNAs *nanos* (*nos*) and *cyclin B* (*cyc B*) organized at the poles of dividing PBs (Gavis, Curtis, & Lehmann, 1996; Raff, Whitfield, & Glover, 1990). A functional role for centrosomes in PGC development was demonstrated years later by pharmacological experiments. Microinjection of the DNA replication inhibitor aphidicolin arrests nuclear divisions and generates a population of anucleated centrosomes that are sufficient to migrate to the posterior pole, recruit germ plasm, and initiate PB formation (Raff & Glover, 1989). In the absence of nuclei, however, these PBs never cellularize. Similar findings were observed by genetic analysis, as loss of the mitotic kinase *pan gu* (*png*) also produces a

population of anucleated centrosomes sufficient to recruit germ plasm and induce PBs (Lerit & Gavis, 2011). These studies demonstrate centrosomes are sufficient to initiate early steps in PGC development.

Pharmacological studies and mutant analysis also indicate that centrosomes are necessary for PGC formation. Treatment with microtubule antagonists acutely blocks or arrests PGC formation depending upon the time of administration (Raff & Glover, 1989). In contrast, loss of the centrosome components Aurora A (AurA), Centrosomin (Cnn), or Transforming acidic coiled-coil (Tacc), or the microtubule motors dynein or Eg5/Klp61F impair the association of germ plasm with centrosomes and its segregation into nascent PBs, leading to an overall reduction in the number of PGCs formed (Lerit et al., 2017; Lerit & Gavis, 2011). Similar defects were also observed following loss of the germ plasm component *germ cell-less*, which contributes to the timely separation of the duplicated centrosomes (Lerit et al., 2017). Finally, live imaging revealed germ plasm transits directly on astral microtubules toward centrosomes (Lerit & Gavis, 2011). Taken together, these studies support a central role for centrosomes in directing multiple distinct steps of PGC development.

The microtubule-nucleating activity of centrosomes is instructed through the pericentriolar material (PCM), a composite of numerous proteins that surrounds the central pair of centrioles (Nigg & Raff, 2009). We recently demonstrated a direct interaction between the PCM components Cnn and Pericentrin (Pcnt)-like-protein (PLP) supports the formation of a centrosome scaffold required to organize the PCM structure (Lerit et al., 2015; Richens et al., 2015). Loss of either *cnn* or *plp* results in similar embryonic defects: disorganized PCM and microtubules, centrosome spacing defects, aberrant spindle formation, and embryonic lethality (Lerit et al., 2015; Megraw, Kilaru, Turner, & Kaufman, 2002). Although Cnn is required for PGC formation, a role for PLP has never been examined.

In this study, we use genetic analysis and quantitative imaging approaches to investigate the requirement of PLP in PGC formation. Our data support a role for PLP at various steps throughout PGC development, including the spatial organization of centrosomes, PB dynamics, and the segregation of germ plasm in proliferating PGCs.

2 | RESULTS

2.1 | PLP promotes PGC formation

To elucidate roles of *plp* in regulating PGC formation during *Drosophila* embryogenesis, we set out to investigate the effects of *plp* depletion on PGC number in NC 13–14 embryos. Due to a pronounced uncoordinated phenotype, null *plp* mutant animals are only partially viable with adults dying shortly after eclosion (Martinez-Campos, Basto, Baker, Kernan, & Raff, 2004). Therefore, to examine a requirement for PLP during stages of PGC formation, we depleted *plp* in the germline using either *nos-GAL4* to drive plp^{RNAi} expression (hereafter, plp^{RNAi}) or germline clone analysis. Expression of plp^{RNAi} resulted in an average of ~50% downregulation of *plp* mRNA in 0–1.5 hr embryos as detected by quantitative polymerase chain reaction (qPCR) (Figure S1a–b”). We note the efficiency of *plp* RNAi knockdown ranged widely, which is likely the result of variable *GAL4* expression levels (Figure S1b–b′). Reducing *plp* expression resulted in a corresponding PGC loss. While control embryos

expressing *mCherry*^{RNAi} under *nos-GAL4* (hereafter, *mCherry*^{RNAi}) formed an average of 31.3 ± 3.1 PGCs (N = 24 embryos), similar to wild-type (WT; 30.4 ± 4.6 PGCs from N = 23 embryos), *plp*^{RNAi} embryos showed significantly fewer PGCs (20.7 ± 7.1 from N = 20 embryos, $p < .0001$) (Figure 1a,b). To confirm this result, we generated *plp* null mutant germline clone embryos (*plp* GLCs) using the FLP/ovoD method (Chou & Perrimon, 1996). Consistently, PGC number was also significantly decreased in *plp* GLC embryos (18.3 ± 9 from N = 23 embryos, $p < .0001$). (Figure 1a,b). These data indicate that depletion of *plp* via RNAi or GLC results in similar reductions in PGC number and raise the possibility that PGC formation may be particularly sensitive to PLP protein dosage.

To examine consequences of PLP dosage, we first evaluated PLP protein levels through quantitative immunoblotting. Consistent with our qPCR analysis, these data show *plp*^{RNAi} resulted in an average of ~50% downregulation of PLP protein, similar to *plp* hemizygotes (*plp*^{2172}/+; Figure 1c,d). In contrast, we were unable to detect PLP protein in *plp* GLCs (Figure 1c,d). To further explore the dose-dependent response of PLP on PGC formation, we quantified PGCs in hemizygous *plp* embryos. For these studies, we examined both *plp*^{2172}/+ and *plp*^{2172}, *FRT2A*/+ embryos to control for the unlikely possibility that the presence of FRT sites may influence PGC number. In both genotypes, halving PLP dosage results in a significant reduction in PGC number relative to WT controls, similar to *plp*^{RNAi} or *plp* GLCs (Figure 1a,b). Taken together, these results suggest that proper PGC formation requires normal levels of PLP protein. Given their similar responses with respect to PLP expression and PGC formation, we interchangeably used *plp*^{RNAi} or *plp* GLC embryos in subsequent experiments.

2.2 | PLP is dispensable for Vas localization

The assembly and localization of the germ plasm to the posterior cortex is critical for PGC formation (Illmensee & Mahowald, 1974). Thus, to understand the molecular mechanisms underlying a requirement for PLP in PGC formation, we first asked whether germ plasm localization is affected in *plp*^{RNAi} embryos by monitoring the expression and localization of Vas (Hay, Jan, & Jan, 1990). Quantitative western blot analysis indicates that Vas expression is unchanged following *plp* depletion (Figure 2a,b). Similarly, immunofluorescence also showed that knockdown of *plp* did not affect germ plasm localization to the posterior cortex (Figure 2c,d). We conclude that PLP is not required for the localization or expression of Vas. These results suggest that early phases of germ plasm assembly, localization, and anchorage to the posterior pole occur normally in the absence of *plp*.

2.3 | PLP promotes PB protrusion during PB budding

PGC formation is characterized by the actin-dependent protrusion of PBs from the posterior embryonic cortex followed by the closure of an actin-rich contractile ring, or PB furrow, at the base of each PB (Warn et al., 1985). Consistent with previous studies, we found that PBs start to protrude from the posterior cortex during NC 10 (Figure 3a) (Raff & Glover, 1989; Williamson & Lehmann, 1996). At this time, over 80% of control *mCherry*^{RNAi} embryos (N = 33 embryos) have PBs (Figure 3a,c). In contrast, we observed an apparent delay in PB protrusion in ~45% age-matched *plp*^{RNAi} embryos (Figure 3a; N = 33 embryos). PB formation is only initiated when centrosomes approach within 5 μm from the posterior pole

(Raff & Glover, 1989). We measured the distance between the posterior cortex and proximal centrosomes in control versus *plp*^{RNAi} embryos to determine if centrosome migration to the posterior was impaired. Quantification showed no difference in the distances of *plp*^{RNAi} centrosomes from the posterior cortex relative to controls during NC 10 (Figure 3a,b). Taken together, these data support a role for PLP in PB formation. That PB formation is delayed despite the correct localization of centrosomes implies that either the physical proximity of the centrosome is insufficient to induce budding and/or the centrosomes from *plp*-depleted animals are not fully functional.

2.4 | PLP is required for centrosome separation

Proper centrosome assembly and function are required for PGC formation (Chodagam, Royou, Whitfield, Karess, & Raff, 2005; Jones & Macdonald, 2015; Lerit et al., 2017; Lerit & Gavis, 2011; Raff & Glover, 1989). During cell-cycle progression, centrosomes duplicate and become fully separated by prophase along with an accompanying increase in microtubule nucleation (Tanenbaum & Medema, 2010). Previous work indicates PLP serves as a centrosome scaffold protein and also contributes to centrosome separation in the soma region of syncytial embryos (Lerit et al., 2015; Richens et al., 2015). A plausible hypothesis, therefore, is that defects in centrosome separation may contribute to the aberrant PB protrusion in *plp* mutants. To test this possibility, we measured the distances between two centrosomes within control and *plp*^{RNAi} embryos during prophase of NC 10 (Figure 4a,b). Normally, centrosomes are completely separated to opposite sides of the nucleus by prophase (Sullivan & Theurkauf, 1995). While the centrosomes of control embryos are fully separated in prophase (10.0 ± 1.0 μm; $N = 49$ centrosome pairs from 12 embryos), loss of *plp* was associated with a significant reduction in the distance between centrosomes (8.9 ± 1.4 μm; $N = 48$ centrosome pairs from 10 embryos, $p < .0001$) (Figure 4a–c). Moreover, while all centrosomes analyzed from control embryos showed centrosome separation distances >8 μm, ~40% of *plp*^{RNAi} centrosome pairs were separated by ≤8 μm (Figure 4c, dashed line). In the representative image shown, centrosome proximity to the posterior cortex and proper centrosome separation appear to be insufficient for PB protrusion in some *plp*^{RNAi} embryos (Figure 4a, *plp*^{RNAi}, dashed lines). These results support a role for PLP in promoting centrosome separation and further highlight the importance of proper centrosome dynamics for PB growth (Lerit et al., 2017).

2.5 | PLP contributes to proper germ plasm distribution

To study the contribution of PLP in mediating germ plasm segregation, we employed a combination of static and live imaging and monitored Vas distribution throughout the processes of PB and PGC formation. During PB formation at NC 10–11, we found robust association of Vas with centrosomes in both control and *plp* GLC embryos (Figure 5a,b). These data indicate germ plasm release from the posterior cortex and trafficking toward nuclei occur normally. In some *plp* GLC embryos, however, Vas appeared less tightly clustered around the PB centrosomes (arrowhead, Figure 5b inset). Similar defects were observed in PB from *plp*^{RNAi} embryos (Figure S2a,b).

During NC 12–13, after PGCs have formed, control embryos typically showed an even, symmetrical enrichment of Vas at the two poles marked by separated centrosomes (Figures

5c and S2c). In contrast, *plp* GLC and plp^{RNAi} embryos show Vas more diffusely spread throughout the PGC (Figures 5d and S2d). We quantified the frequency of abnormal Vas distribution within control PGCs and found $N = 3/198$ PGCs with abnormal Vas from 15 $mCherry^{RNAi}$ embryos and $N = 2/146$ PGCs with abnormal Vas from 11 WT embryos. In contrast, ~80% of plp^{RNAi} embryos showed irregular Vas distributions within their PGCs. Within a given plp^{RNAi} PGC cluster, an average of 20% of PGCs had some Vas remaining dispersed within the cytoplasm instead of closely associated with the centrosomes ($N = 20/122$ PGCs with abnormal Vas from 15 plp^{RNAi} embryos). Similar defects were observed in PGCs from *plp* GLC embryos ($N = 35/169$ PGCs with abnormal Vas from 16 *plp* GLC embryos). These data suggest that PLP is required for Vas to tightly associate with centrosomes and imply that Vas may fail to be evenly to the two daughter cells following PGC proliferation. Consistent with this idea, depletion of PLP by either method resulted in uneven intensities of Vas signal within PGC clusters (asterisks, Figure S2d). We conclude that PLP promotes the efficient segregation of Vas during PGC formation and proliferation.

To examine Vas distribution in greater detail, we monitored the distribution of GFP-Vas by time-lapse imaging in 1–2 hr embryos. In PBs from control embryos, Vas was symmetrically distributed with bilateral concentrations at the presumptive centrosomes (Figures 5e, S2e, Video S1). Similar patterns of Vas distribution were observed in nascent PBs and early PGCs for $N = 5/5$ control embryos. In contrast, irregular Vas distribution was noted in $N = 4/6$ *plp* GLC embryos with Vas loosely associated at nuclei poles (arrowhead, Figure 5e) and/or the inefficient association of Vas granules at nuclei (arrows, Figure 5e, Video S2). Note that in the representative movie shown, PB formation is delayed relative to controls in age-matched *plp* GLCs (Figure 5e, 0:00, and Videos S1, S2). The aberrant incorporation of germ plasm into PBs suggests that some PGCs may fail to inherit the critical threshold of germ plasm required for PGC development (Ewen-Campen et al., 2010). These data suggest that PLP is required for the segregation of the germ plasm into PGCs, likely through a requirement of PLP in supporting a robust astral microtubule array.

2.6 | PLP instructs microtubule organization

Our prior work indicates that *plp* GLC embryos maintain robust microtubule nucleation, yet they exhibit a notable reduction in the radial organization of astral microtubules associated with somatic nuclei (Lerit et al., 2015). In that work, we did not examine the organization of microtubules within PGCs. To further define the role of PLP in PGC development, we visualized microtubule organization in PBs by staining NC 11 embryos for α-Tubulin (α-Tub). Control embryos show astral microtubules are normally organized with a fairly symmetric radial array focused around the centriole marker Asl (Figure 6a, WT). In contrast, the astral microtubules from many *plp* GLC PBs were less organized, as evidenced by discontinuities in the microtubule array, the appearance of microtubule crossover events, and loss of the overall radial symmetry (Figure 6a, *plp* GLC). To quantify the relative organization of microtubules around PB centrosomes, we employed a recently developed semiautomated software (Martin, Veloso, Wu, Katrukha, & Akhmanova, 2018). Through blinded analysis, segmented astral microtubules (Figure 6a, middle row) were separated into radial versus nonradial components using the Asl-labeled centriole as the central reference point (Figure 6a, bottom row). Quantification shows an increase in the microtubule

disorganization in *plp* GLCs, which we display as the percent of nonradial microtubules per centrosome (Figure 6b). These results suggest that PLP is required to support microtubule organization in PGCs, similar to its role in the soma. However, these studies cannot differentiate whether PLP is required to establish or maintain microtubule organization.

To mechanistically address how loss of *plp* disrupts microtubule assembly, we examined the distribution of Cnn at PB centrosomes in control versus *plp* GLC embryos. Cnn is a core component of a PCM scaffold required for centrosome and microtubule organization (Conduit, Brunk, et al., 2010; Conduit, Feng, et al., 2014; Lerit et al., 2015; Megraw, Li, Kao, & Kaufman, 1999; Richens et al., 2015). In control PBs, Cnn radiates from interphase centrosomes (Figure 6c, WT interphase), similar to the Cnn flares previously described in the soma (Megraw et al., 2002). As PBs enter mitosis, Cnn becomes more compactly organized about the centrosome (Figure 6c, WT mitosis). In contrast, the distribution of Cnn appears more disorganized in interphase and mitotic *plp* GLC PBs with Cnn flares appearing more reticulated and fragmented and puncta of Cnn dispersed within the cytosol (Figure 6c, *plp* GLC). Disorganized Cnn was observed at every *plp* GLC centrosome examined ($N > 30$ centrosomes from $N > 10$ embryos). These data suggest that PLP contributes to proper PGC development by regulating MT organization through maintenance of the Cnn-dependent centrosome scaffold.

3 | DISCUSSION

Centrosomes are microtubule organizing centers required for error-free mitosis, and centrosome integrity is important for embryo development across metazoan species (Gonczy & Rose, 2005; Gueth-Hallonet et al., 1993; Kubiak & Prigent, 2012; Rothwell & Sullivan, 1999; Schatten & Sun, 2012). Pcnt was originally identified based on its localization to the PCM and its requirement to organize microtubule arrays in *Xenopus* extracts and cultured human cells (Doxsey, Stein, Evans, Calarco, & Kirschner, 1994). Indeed, chief among the conserved Pcnt functions are its roles in scaffolding the PCM and organizing microtubules (C.-T. Chen et al., 2014; P. Chen et al., 2012; Haren, Stearns, & Lüders, 2009; Lee & Rhee, 2011; Lerit et al., 2015; Lin et al., 2014; Martinez-Campos et al., 2004; Richens et al., 2015; Zimmerman, Sillibourne, Rosa, & Doxsey, 2004). However, relatively little is known about Pcnt function in germline development outside of the role for its ortholog, PLP, in supporting spermatogenesis in *Drosophila* (Galletta et al., 2014; Martinez-Campos et al., 2004; Roque, Saurya, Pratt, Johnson, & Raff, 2018).

While accumulating evidence supports a central role for centrosomes in PGC development, the precise requirements for individual centrosome factors remains relatively unknown. In this study, we assess the requirement of PLP to promote PGC formation. Our data support a model where PLP functions to maintain the Cnn scaffold required for robust organization of the astral microtubule array. Organized microtubules, in turn, are required to promote centrosome separation, recruit germ plasm, induce timely PB protrusion, and instruct germ plasm distribution within proliferating PGCs (Figure 7). Thus, PLP function is required at multiple discrete steps throughout PGC development.

The well-conserved role of Pcnt/PLP in mediating microtubule organization suggests that PLP functions primarily to maintain the microtubule array and promote PGC formation. However, the decreased frequency of PB protrusion in *plp*-depleted embryos is suggestive of an apparent delay in the actin rearrangements that drive this process. Work in several model systems demonstrates crosstalk between centrosomes and the actin cytoskeleton, hinting that microtubule defects may lie at the root of impaired PB formation. For example, actin and microtubules coordinate the nuclear migration and regular spacing in early *Drosophila* embryos. Upon their arrival at the embryo surface, individual nuclei and their associated centrosomes organize independent cytoskeletal arrays (Karr & Alberts, 1986; Schejter & Wieschaus, 1993; von Dassow & Schubiger, 1994). During somatic nuclear divisions, centrosomes coordinate the formation of actin caps during interphase and metaphase furrows during mitosis (Foe & Alberts, 1983; Karr & Alberts, 1986; Sullivan & Theurkauf, 1995). These cycles continue throughout the syncytial blastoderm divisions (Rothwell & Sullivan, 1999). The initial actin and myosin-mediated protrusion of PBs resembles somatic protrusions with the important distinction that PBs do not normally regress. This distinction requires the activity of actin-regulatory proteins, and their loss results in PBs that fail to cellularize (Afshar, Stuart, & Wasserman, 2000). Taken together, our data are consistent with the idea that PLP functions primarily through its role in microtubule organization and may additionally impinge upon the cortical actin network, perhaps indirectly through the microtubules themselves.

PBs derived from anucleated centrosomes fail to cellularize, indicating centrosome-nucleated microtubules are sufficient for early steps leading up to PGC formation, yet insufficient to trigger cytokinesis. Our present work suggests that loss of PLP impairs early steps of PGC development. Clearly, subsets of *plp*-depleted PGCs do cellularize, which is consistent with the idea that these centrosomes are partially functional. These findings are intriguing given the fact that microtubules have a conserved role in triggering events leading to the actin-dependent process of cytokinesis; for example, by directing contractile ring assembly and regulating the contractility of the surrounding cortex (Murthy & Wadsworth, 2008). In accordance, inhibition of microtubules through antagonizing drugs blocks cytokinesis, a result recapitulated in nascent PGCs (Lerit & Gavis, 2011; Raff & Glover, 1989). Therefore, the interplay between microtubules and actin required for PGC development is complex and remains incompletely understood. Nonetheless, the centrosome and its associated factors appear to play a central role in ensuring germline development.

Our finding that PGC formation is particularly sensitive to PLP dosage was unexpected. Null *plp* mutations and deficiency stocks (i.e., chromosomal deletions) may be stably maintained over balancer chromosomes. Thus, while *plp* is clearly not haploinsufficient with respect to viability or fertility, *plp* hemizygotes do show reduced PGC numbers in NC 13–14 embryos. Dose-dependent phenotypes have been reported for other *Drosophila* genes. For example, *oo18 RNA-binding protein* (*orb*) is haploinsufficient for dorsal-ventral axis patterning (Costa et al., 2005). While it is unclear why halving PLP dose disrupts aspects of PGC development, one possibility is that *plp* hemizygotes construct a compromised centrosome scaffold or otherwise fail to maintain robust centrosome functions key to PGC formation/maintenance.

4 | METHODS

4.1 | Fly stocks

The following transgenic lines were used: $y^1 w^{1118}$ was used as the WT control unless otherwise noted; plp^{RNAi} (P{TRiP.HMC05936}^{attP40}; BDSC #65231) and $mCherry^{RNAi}$ (P{Valium20-mCherry}^{attP2}; BDSC #35785) were driven by *nos-GAL4:VP16* (Doren, Williamson, & Lehmann, 1998). GFP-Vas expresses Vas under endogenous regulatory elements (Johnstone & Lasko, 2004). Null *plp* mutant germline clones were generated by the FLP/ovoD method (Chou & Perrimon, 1996) using *FRT2A*, plp^{2172} recombinant chromosomes (Lerit et al., 2015). All strains were maintained using standard laboratory conditions and crosses were maintained at 25°C in a light and temperature-controlled incubator.

4.2 | RNA extraction and qRT-PCR

Two to five milligrams of dechorionated embryos (0–1.5 hr) were collected and used for RNA extraction. RNA was extracted with TRIzol (ThermoFisher) and then treated with TURBO DNase (Thermo, AM2238) prior to RT-PCR. Five hundred nanograms of RNA was reverse transcribed to cDNA with Superscript IV (Thermo). The qPCR was performed on a Bio-Rad CFX96 Real-time system with iTaq Universal SYBR Green Supermix (Bio-Rad). Values were normalized to *RP49* expression levels. Ct values from the qPCR results were analyzed and the relative expression levels for each condition were calculated using Microsoft Excel. The primers used in this study are listed below:

rp49 Forward: CATACAGGCCCAAGATCGTG

rp49 Reverse: ACAGCTTAGCATATCGATCCG

plp Foward: CGCAGCAAGGAGGAGATAAC

plp Reverse: TCAGCCTGCAGTTTGTTCAC

4.3 | Western blotting

Five milligrams of embryos were lysed in 100 μl 0.1% PBST (PBS supplemented with 0.1% Tween-20) and homogenized with a 1 ml glass dounce (Wheaton), 30 μl 5X SDS loading dye was added into the total protein extract and the samples were boiled at 95°C for 10 min. Samples were run on an SDS-PAGE gel and transferred onto a nitrocellulose membrane with a Trans-Blot Turbo Blotting system (Bio-Rad). To analyze PLP, ~10 μl of paraformaldehyde-fixed embryos were lysed in 150 μl 0.1% PBST. Samples were transferred onto a nitrocellulose membrane with a traditional wet-transfer buffer supplemented with 0.02% SDS. The following primary antibodies were used: rabbit anti-PLP (1:4000, gift from N. Rusan, NIH), rat anti-Vasa (1:100, DSHB; A. Spradling, Carnegie Institute), mouse anti-Khc SUK 4 (1:200, DSHB; J.M. Scholey, University of Colorado), mouse anti-β-Tubulin E7 (1:1000, DSHB; M. Klymkowsky, University of Colorado). Secondary antibodies: goat anti-mouse HRP (1:5000, ThermoFisher #31430) and goat anti-rat IgG HRP (1:5000, Caltag Medsystems #6908–250). Densitometry was measured in Adobe Photoshop.

4.4 | Fixed immunofluorescence

Embryos were fixed in a 1:4 solution of 4% paraformaldehyde: heptane for 20 min and devitellinized in methanol. For visualization of MTs, embryos were prepared as previously described (Theurkauf, 1994). Briefly, embryos were fixed in a 1:1 mixture of 37% paraformaldehyde: heptane for 3 min, rinsed in PBS, and manually devitellinized using 30G PrecisionGlide needles (BD). Embryos were blocked in BBT buffer (PBS supplemented with 0.1% BSA and 0.1% Tween-20); for Asl staining, 0.5% BSA was used. Samples were incubated overnight at 4°C with primary antibody in BBT, further blocked in BBT supplemented with 2% normal goat serum, and incubated for 2 hr at room temperature with secondary antibody with DAPI. Embryos were mounted in Aqua-Poly/Mount (Polysciences, Inc.) prior to imaging.

The following primary antibodies were used: rabbit anti-Vas (1:2000, gift from P. Lasko, McGill University), rat anti-Vas (1:10, DSHB), guinea pig anti-Asl (1:4000, gift from G. Rogers, University of Arizona), mouse anti-α-Tubulin DM1α (1:500, Sigma-Aldrich T6199), rabbit anti-phospho-Histone H3 Ser10 (pH3; 1:1000, Millipore 05–570), mouse anti-phospho-Tyrosine 4G10 (pTyr; 1:1000, Millipore 05–321), Alexa 568 conjugated phalloidin (Invitrogen #12380). Secondary antibodies: Alexa Fluor 488, 568, or 647 (1:500, Molecular Probes), and DAPI (10 ng/ml, ThermoFisher).

4.5 | Live imaging

Embryos were prepared for live imaging as described in (Lerit et al., 2017). Briefly, dechorionated embryos were adhered to a sticky 22 × 30 mm # 1.5 glass coverslip and covered with a thin layer of halocarbon oil. Imaging of GFP-Vas was captured at 1 μm z-intervals over a 10–15 μm volume at 20 s intervals.

4.6 | Microscopy

Images were acquired on a Nikon Ti-E system fitted with a Yokagawa CSU-X1 spinning disk head, Hamamatsu Orca Flash 4.0 v2 digital CMOS camera, Perfect Focus system, Nikon LU-N4 solid state laser launch (15 mW 405, 488, 561, and 647 nm) using high NA objectives, ×100, 1.49 NA Apo TIRF oil immersion; ×40, 1.3 NA Plan Fluor oil immersion all powered through Nikon Elements AR software on a 64-bit HP Z440 workstation.

4.7 | Image analysis

ImageJ (NIH) was used for all image analysis. The distance between two centrosomes was measured from embryos in NC 10 prophase by using the line tool. When two centrosomes were not present within the same focal plane, we calculated the distance as the hypotenuse between the centrosomes in a 3D volume. The line tool in ImageJ was also used to measure the distance between centrosomes and the posterior cortex in NC 10 embryos using maximum intensity projected images. Microtubule organization was analyzed using the FeatureJ plugin for ImageJ and a customized ImageJ macro (nonradiality map), as previously reported (Martin et al., 2018). This tool was used to split single optical frame images of segmented microtubules into radial versus nonradial components based on microtubule orientation in relation to a user-defined central point (here, peak Asl fluorescence). The resulting nonradial heat maps were used to quantify the ratio of nonradial

microtubules relative to the total microtubule signal from the original segmented images. To do the MT segmentation, we employed a Python-based script run in the Jupyter Notebook, as previously reported (J. Chen et al., 2018). Vas levels were calculated from a region-of-interest at the posterior pole and background subtracted using an equal area from a soma region within the same image

Images were assembled using ImageJ (NIH), QuickTime Player Pro 7 (Apple), and Adobe Photoshop and Illustrator software to crop regions of interest, adjust brightness and contrast, generate maximum-intensity projections, separate or merge channels, and assemble time-lapse images.

4.8 | Statistical methods

Data were plotted and statistical analysis was performed using GraphPad Prism software. To calculate significance, distribution normality was first confirmed with a D'Agnostino and Pearson normality test. Data were then analyzed by Student's two-tailed *t* test or a nonparametric Mann–Whitney test and are displayed as mean ± *SD*. Data shown are representative results from at least two independent experiments, as indicated in the figure legends.

Supplementary Material

Refer to Web version on PubMed Central for supplementary material.

ACKNOWLEDGMENTS

Stocks obtained from the Bloomington *Drosophila* Stock Center (NIH P40OD018537) were used in this study. Antibodies from the Developmental Studies Hybridoma Bank, created by the NICHD of the NIH and maintained at the University of Iowa Department of Biology were used. For reagents, we thank Drs. Greg Rogers, Nasser Rusan, and Andrew Kowalczyk. Jingsheng Gu provided fly media. We thank Dr. Pearl Ryder for help with blinded analysis. We thank Dr. Girish Deshpande and members of the Lerit lab for critical reading of this manuscript. We are grateful to Holly Jordan for early observations that initiated this project. This work was supported by Emory University School of Medicine Development Funds and NIH grant 5K22HL126922 to DAL.

Funding information

National Institutes of Health, Grant/Award Number: 5K22HL126922; Emory University School of Medicine Development Funds

REFERENCES

Afshar K, Stuart B, & Wasserman SA (2000). Functional analysis of the Drosophila diaphanous FH protein in early embryonic development. Development, 127(9), 1887–1897. [PubMed: 10751177]

Benner L, Deshpande G, & Lerit DA (2018). Primordial germ cells of *Drosophila melanogaster*. In Skinner MK (Ed.), Encyclopedia of reproduction (Second ed., pp. 145–151). Oxford: Academic Press.

Breitwieser W, Markussen FH, Horstmann H, & Ephrussi A (1996). Oskar protein interaction with Vasa represents an essential step in polar granule assembly. Genes & Development, 10(17), 2179–2188. [PubMed: 8804312]

Chen C-T, Hehnly H, Yu Q, Farkas D, Zheng G, Redick SD, … Doxsey S (2014). A unique set of centrosome proteins requires pericentrin for spindle-pole localization and spindle orientation. Current Biology: CB, 24(19), 2327–2334. 10.1016/j.cub.2014.08.029 [PubMed: 25220058]

Chen J, Ding L, Viana MP, Hendershott MC, Yang R, Mueller IA, & Rafelski SM (2018). The Allen Cell Structure Segmenter: A new open source toolkit for segmenting 3D intracellular structures in fluorescence microscopy images. bioRxiv, 491035. 10.1101/491035

Chen P, Gao R, Chen S, Pu L, Li P, Huang Y, & Lu L (2012). A pericentrin-related protein homolog in *Aspergillus nidulans* plays important roles in nucleus positioning and cell polarity by affecting microtubule organization. Eukaryotic Cell, 11(12), 1520–1530. 10.1128/EC.00203-12 [PubMed: 23087372]

Chodagam S, Royou A, Whitfield W, Karess R, & Raff JW (2005). The centrosomal protein CP190 regulates myosin function during early Drosophila development. Current Biology, 15(14), 1308–1313. 10.1016/j.cub.2005.06.024 [PubMed: 16051175]

Chou T-B, & Perrimon N (1996). The autosomal FLP-DFS technique for generating Germline mosaics in >*Drosophila melanogaster*. Genetics, 144(4), 1673. [PubMed: 8978054]

Cinalli RM, & Lehmann R (2013). A spindle-independent cleavage pathway controls germ cell formation in drosophila. Nature Cell Biology, 15 (7), 839–845. 10.1038/ncb2761 [PubMed: 23728423]

Conduit PT, Brunk K, Dobbelaere J, Dix CI, Lucas EP, & Raff JW (2010). Centrioles regulate centrosome size by controlling the rate of Cnn incorporation into the PCM. Current Biology, 20(24), 2178–2186. 10.1016/j.cub.2010.11.011 [PubMed: 21145741]

Conduit PT, Feng Z, Richens JH, Baumbach J, Wainman A, Bakshi SD, … Raff JW (2014). The centrosome-specific phosphorylation of Cnn by polo/Plk1 drives Cnn scaffold assembly and centrosome maturation. Developmental Cell, 28(6), 659–669. 10.1016/j.devcel.2014.02.013 [PubMed: 24656740]

Costa A, Wang Y, Dockendorff TC, Erdjument-Bromage H, Tempst P, Schedl P, & Jongens TA (2005). The drosophila fragile X protein functions as a negative regulator in the orb autoregulatory pathway. Developmental Cell, 8(3), 331–342. [PubMed: 15737929]

Counce SJ (1963). Developmental morphology of polar granules in Drosophila. Including observations on pole cell behavior and distribution during embryogenesis. Journal of Morphology, 112(2), 129–145. 10.1002/jmor.1051120203

Doren MV, Williamson AL, & Lehmann R (1998). Regulation of zygotic gene expression in Drosophila primordial germ cells. Current Biology, 8(4), 243–246. 10.1016/S0960-9822(98)70091-0 [PubMed: 9501989]

Doxsey SJ, Stein P, Evans L, Calarco PD, & Kirschner M (1994). Pericentrin, a highly conserved centrosome protein involved in microtubule organization. Cell, 76(4), 639–650. 10.1016/0092-8674(94)90504-5 [PubMed: 8124707]

Ewen-Campen B, Schwager EE, & Extavour CGM (2010). The molecular machinery of germ line specification. Molecular Reproduction and Development, 77(1), 3–18. 10.1002/mrd.21091 [PubMed: 19790240]

Foe VE, & Alberts BM (1983). Studies of nuclear and cytoplasmic behaviour during the five mitotic cycles that precede gastrulation in Drosophila embryogenesis. Journal of Cell Science, 61(1), 31. [PubMed: 6411748]

Forrest KM, & Gavis ER (2003). Live imaging of endogenous RNA reveals a diffusion and entrapment mechanism for nanos mRNA localization in Drosophila. Current Biology, 13(14), 1159–1168. 10.1016/S0960-9822(03)00451-2 [PubMed: 12867026]

Galletta BJ, Guillen RX, Fagerstrom CJ, Brownlee CW, Lerit DA, Megraw TL, … Bettencourt-Dias M (2014). Drosophila pericentrin requires interaction with calmodulin for its function at centrosomes and neuronal basal bodies but not at sperm basal bodies. Molecular Biology of the Cell, 25(18), 2682–2694. 10.1091/mbc.e13-10-0617 [PubMed: 25031429]

Gavis ER, Curtis D, & Lehmann R (1996). Identification of cis-acting sequences that Control nano sRNA localization. Developmental Biology, 176(1), 36–50. 10.1006/dbio.1996.9996 [PubMed: 8654893]

Gonczy P, & Rose LS (2005). Asymmetric cell division and axis formation in the embryo the C. elegans research community. WormBook, 1551–8507. 10.1895/wormbook.1.30.1, http://www.wormbook.org

Gueth-Hallonet C, Antony C, Aghion J, Santa-Maria A, Lajoie-Mazenc I, Wright M, & Maro B (1993). Gamma-tubulin is present in acentriolar MTOCs during early mouse development. Journal of Cell Science, 105(1), 157. [PubMed: 8360270]

Haren L, Stearns T, & Lüders J (2009). Plk1-dependent recruitment of γ-tubulin complexes to mitotic centrosomes involves multiple PCM components. PLoS One, 4(6), e5976. 10.1371/journal.pone.0005976 [PubMed: 19543530]

Hay B, Jan LY, & Jan YN (1990). Localization of vasa, a component of drosophila polar granules, in maternal-effect mutants that alter embryonic anteroposterior polarity. Development, 109(2), 425–433. [PubMed: 2119289]

Illmensee K, & Mahowald AP (1974). Transplantation of posterior polar plasm in Drosophila. Induction of germ cells at the anterior pole of the egg. Proceedings of the National Academy of Sciences of the United States of America, 71(4), 1016–1020. [PubMed: 4208545]

Johnstone O, & Lasko P (2004). Interaction with eIF5B is essential for vasa function during development. Development, 131(17), 4167–4178. 10.1242/dev.01286 [PubMed: 15280213]

Jones J, & Macdonald PM (2015). Neurl4 contributes to germ cell formation and integrity in Drosophila. Biology Open, 4(8), 937–946. 10.1242/bio.012351 [PubMed: 26116656]

Karr TL, & Alberts BM (1986). Organization of the cytoskeleton in early Drosophila embryos. The Journal of Cell Biology, 102(4), 1494–1509. 10.1083/jcb.102.4.1494 [PubMed: 3514634]

Kubiak JZ, & Prigent C (2012). The centrosome life story in Xenopuslaevis. In Schatten H (Ed.), The centrosome: Cell and molecular mechanisms of functions and dysfunctions in disease (pp. 347–363). Totowa, NJ: Humana Press.

Lantz VA, Clemens SE, & Miller KG (1999). The actin cytoskeleton is required for maintenance of posterior pole plasm components in the Drosophila embryo. Mechanisms of Development, 85(1), 111–122. 10.1016/S0925-4773(99)00096-9 [PubMed: 10415352]

Lee K, & Rhee K (2011). PLK1 phosphorylation of pericentrin initiates centrosome maturation at the onset of mitosis. The Journal of Cell Biology, 195(7), 1093–1101. 10.1083/jcb.201106093 [PubMed: 22184200]

Lehmann R (2016). Chapter thirty-nine - Germ plasm biogenesis—An Oskar-centric perspective. In Wassarman PM (Ed.), Current topics in developmental biology (Vol. 116, pp. 679–707). Cambridge, MA: Academic Press. 10.1016/bs.ctdb.2015.11.024 [PubMed: 26970648]

Lehmann R, & Nüsslein-Volhard C (1986). Abdominal segmentation, pole cell formation, and embryonic polarity require the localized activity of Oskar, a maternal gene in drosophila. Cell, 47(1), 141–152. 10.1016/0092-8674(86)90375-2 [PubMed: 3093084]

Lerit DA, & Gavis ER (2011). Transport of germ plasm on astral microtubules directs germ cell development in Drosophila. Current Biology: CB, 21(6), 439–448. 10.1016/j.cub.2011.01.073 [PubMed: 21376599]

Lerit DA, Jordan HA, Poulton JS, Fagerstrom CJ, Galletta BJ, Peifer M, & Rusan NM (2015). Interphase centrosome organization by the PLP-Cnn scaffold is required for centrosome function. The Journal of Cell Biology, 210(1), 79–97. 10.1083/jcb.201503117 [PubMed: 26150390]

Lerit DA, Shebelut CW, Lawlor KJ, Rusan NM, Gavis ER, Schedl P, & Deshpande G (2017). Germ cell-less promotes centrosome segregation to induce germ cell formation. Cell Reports, 18(4), 831–839. 10.1016/j.celrep.2016.12.074 [PubMed: 28122234]

Lin T. c., Neuner A, Schlosser YT, Scharf AND, Weber L, & Schiebel E (2014). Cell-cycle dependent phosphorylation of yeast pericentrin regulates γ-TuSC-mediated microtubule nucleation. eLife, 3, e02208. 10.7554/eLife.02208 [PubMed: 24842996]

Mahowald AP (1962). Fine structure of pole cells and polar granules in *Drosophila melanogaster*. Journal of Experimental Zoology, 151(3), 201–215. 10.1002/jez.1401510302

Mahowald AP (2001). Assembly of the Drosophila germ plasm. In International review of cytology (Vol. 203, pp. 187–213). San Diego, CA: Academic Press. [PubMed: 11131516]

Martin M, Veloso A, Wu J, Katrukha EA, & Akhmanova A (2018). Control of endothelial cell polarity and sprouting angiogenesis by non-centrosomal microtubules. eLife, 7, e33864. 10.7554/eLife.33864 [PubMed: 29547120]

Martinez-Campos M, Basto R, Baker J, Kernan M, & Raff JW (2004). The drosophila pericentrin-like protein is essential for cilia/flagella function, but appears to be dispensable for mitosis. The Journal of Cell Biology, 165(5), 673–683. [PubMed: 15184400]

Megraw TL, Kilaru S, Turner FR, & Kaufman TC (2002). The centrosome is a dynamic structure that ejects PCM flares. Journal of Cell Science, 115(23), 4707–4718. 10.1242/jcs.00134 [PubMed: 12415014]

Megraw TL, Li K, Kao LR, & Kaufman TC (1999). The centrosomin protein is required for centrosome assembly and function during cleavage in Drosophila. Development, 126(13), 2829–2839. [PubMed: 10357928]

Murthy K, & Wadsworth P (2008). Dual role for microtubules in regulating cortical contractility during cytokinesis. Journal of Cell Science, 121 (Pt 14), 2350–2359. 10.1242/jcs.027052 [PubMed: 18559890]

Nigg EA, & Raff JW (2009). Centrioles, centrosomes, and cilia in health and disease. Cell, 139(4), 663–678. 10.1016/j.cell.2009.10.036 [PubMed: 19914163]

Padash Barmchi M, Rogers S, & Häcker U (2005). DRhoGEF2 regulates actin organization and contractility in the Drosophila blastoderm embryo. The Journal of Cell Biology, 168(4), 575–585. 10.1083/jcb.200407124 [PubMed: 15699213]

Raff JW, & Glover DM (1989). Centrosomes, and not nuclei, initiate pole cell formation in Drosophila embryos. Cell, 57(4), 611–619. 10.1016/0092-8674(89)90130-X [PubMed: 2497990]

Raff JW, Whitfield WG, & Glover DM (1990). Two distinct mechanisms localise cyclin B transcripts in syncytial Drosophila embryos. Development, 110(4), 1249–1261. [PubMed: 2151612]

Richens JH, Barros TP, Lucas EP, Peel N, Pinto DMS, Wainman A, & Raff JW (2015). The Drosophila pericentrin-like-protein (PLP) cooperates with Cnn to maintain the integrity of the outer PCM. Biology Open, 4(8), 1052–1061. 10.1242/bio.012914 [PubMed: 26157019]

Roque H, Saurya S, Pratt MB, Johnson E, & Raff JW (2018). Drosophila PLP assembles pericentriolar clouds that promote centriole stability, cohesion and MT nucleation. PLoS Genetics, 14(2), e1007198. 10.1371/journal.pgen.1007198 [PubMed: 29425198]

Rothwell WF, & Sullivan W (1999). The centrosome in early drosophila embryogenesis. In Palazzo RE & Schatten GP (Eds.), Current topics in developmental biology (Vol. 49, pp. 409–447). Cambridge, MA: Academic Press. 10.1016/s0070-2153(99)49020-9

Schatten H, & Sun Q-Y (2012). Nuclear–centrosome relationships during fertilization, cell division, embryo development, and in somatic cell nuclear transfer embryos. In Schatten H (Ed.), The centrosome: Cell and molecular mechanisms of functions and dysfunctions in disease (pp. 59–72). Totowa, NJ: Humana Press.

Schejter ED, & Wieschaus E (1993). Functional elements of the cytoskeleton in the early Drosophila embryo. Annual Review of Cell Biology, 9(1), 67–99. 10.1146/annurev.cb.09.110193.000435

Sinsimer KS, Lee JJ, Thiberge SY, & Gavis ER (2013). Germ plasm anchoring is a dynamic state that requires persistent trafficking. Cell Reports, 5(5), 1169–1177. 10.1016/j.celrep.2013.10.045 [PubMed: 24290763]

Sullivan W, & Theurkauf WE (1995). The cytoskeleton and morphogenesis of the early Drosophila embryo. Current Opinion in Cell Biology, 7 (1), 18–22. 10.1016/0955-0674(95)80040-9 [PubMed: 7755985]

Tanenbaum ME, & Medema RH (2010). Mechanisms of centrosome separation and bipolar spindle assembly. Developmental Cell, 19(6), 797–806. 10.1016/j.devcel.2010.11.011 [PubMed: 21145497]

Theurkauf WE (1994). Chapter 25 immunofluorescence analysis of the cytoskeleton during oogenesis and early embryogenesis. In Goldstein LSB & Fyrberg EA (Eds.), Methods in cell biology (Vol. 44, pp. 489–505). San Diego, CA: Academic Press. [PubMed: 7707968]

Vanzo N, Oprins A, Xanthakis D, Ephrussi A, & Rabouille C (2007). Stimulation of endocytosis and actin dynamics by Oskar polarizes the Drosophila oocyte. Developmental Cell, 12(4), 543–555. 10.1016/j.devcel.2007.03.002 [PubMed: 17419993]

von Dassow G, & Schubiger G (1994). How an actin network might cause fountain streaming and nuclear migration in the syncytial Drosophila embryo. The Journal of Cell Biology, 127(6 Pt 1), 1637–1653. 10.1083/jcb.127.6.1637 [PubMed: 7798318]

Warn RM, Smith L, & Warn A (1985). Three distinct distributions of F-actin occur during the divisions of polar surface caps to produce pole cells in Drosophila embryos. The Journal of Cell Biology, 100(4), 1010–1015. 10.1083/jcb.100.4.1010 [PubMed: 3980576]

Williamson A, & Lehmann R (1996). Germ cell development in Drosophila. Annual Review of Cell and Developmental Biology, 12(1), 365–391. 10.1146/annurev.cellbio.12.1.365

Zimmerman WC, Sillibourne J, Rosa J, & Doxsey SJ (2004). Mitosis-specific anchoring of γ tubulin complexes by pericentrin controls spindle organization and mitotic entry. Molecular Biology of the Cell, 15(8), 3642–3657. 10.1091/mbc.e03-11-0796 [PubMed: 15146056]

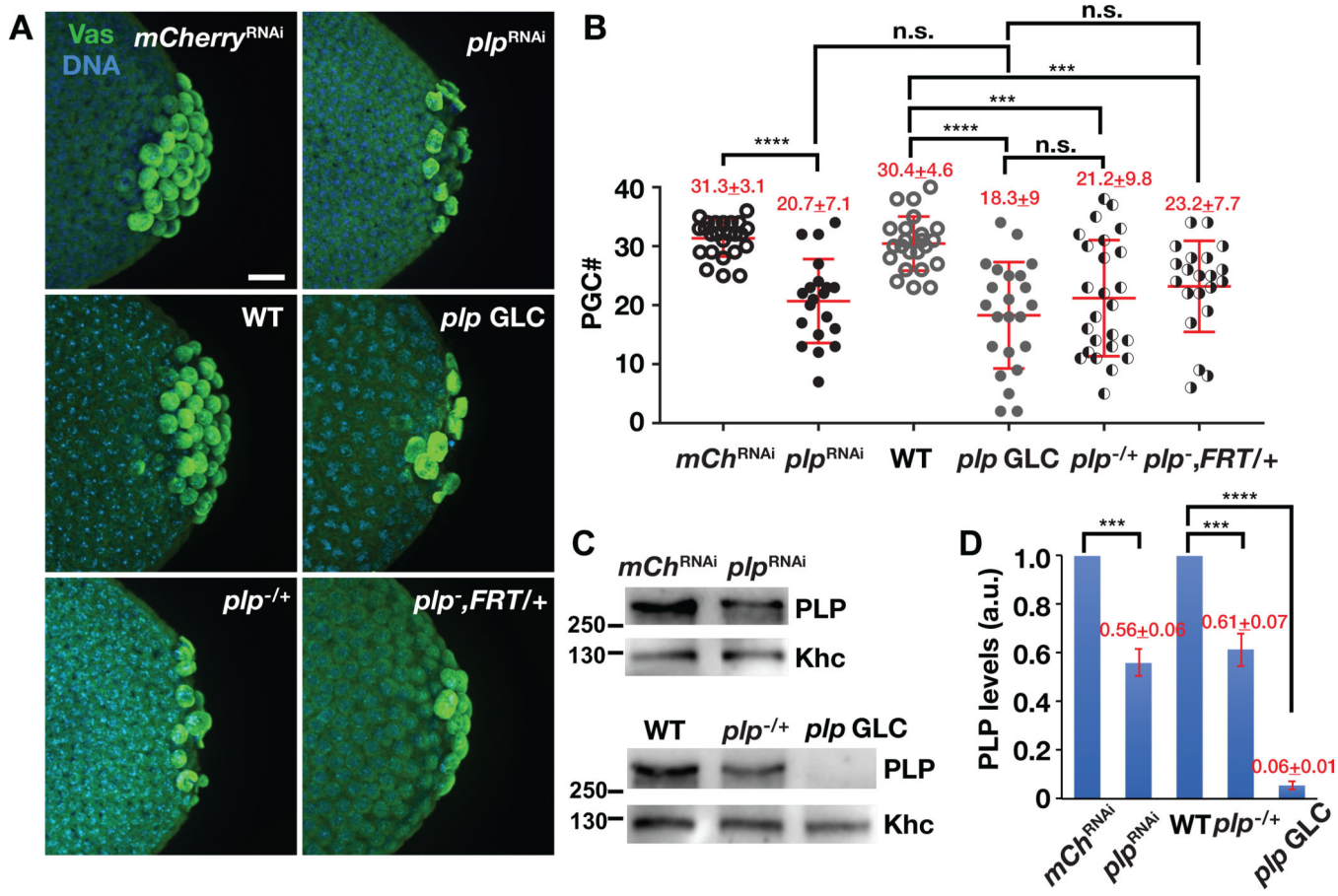

FIGURE 1.

PLP promotes PGC formation. (a) Images show maximum-intensity projections of NC 13–14 embryos of the indicated genotypes stained with anti-Vas (green) to label PGCs. In this and all images, posterior is to the right. Bar, 10 μm. (b) Quantification of PGCs from NC 13–14 embryos. Each data point represents one embryo. Mean ± *SD* PGCs are displayed (red). mCh^{RNAi} ($mCherry^{RNAi}$, $N = 24$ embryos); plp^{RNAi} ($N = 20$ embryos); WT ($N = 23$ embryos); *plp* GLC ($N = 23$ embryos); *plp*−/+ (plp^{2172}/+; $N = 25$ embryos); *plp*−, *FRT*/+ (plp^{2172},*FRT2A*/+, $N = 21$ embryos). ****$p < .0001$, ***$p < .001$, n.s., not significant by Student's *t* test. The experiment was performed twice with similar results. (c) Western blot analysis of PLP expression from 0 −2 hr embryo extracts of the indicated genotypes. Anti-Khc antibodies were used for normalization. (d) Densitometry quantification of PLP levels from western blot analysis. PLP expression values are relative to the loading control, anti-Khc, and normalized to the $mCherry^{RNAi}$ or WT. Mean ± *SD* from three replicates are displayed (red). a.u., arbitrary units; ****$p < .001$, ***$p < .001$ by Student's *t* test. PGC, primordial germ cells; PLP, Pericentrin-like protein; WT, wild-type

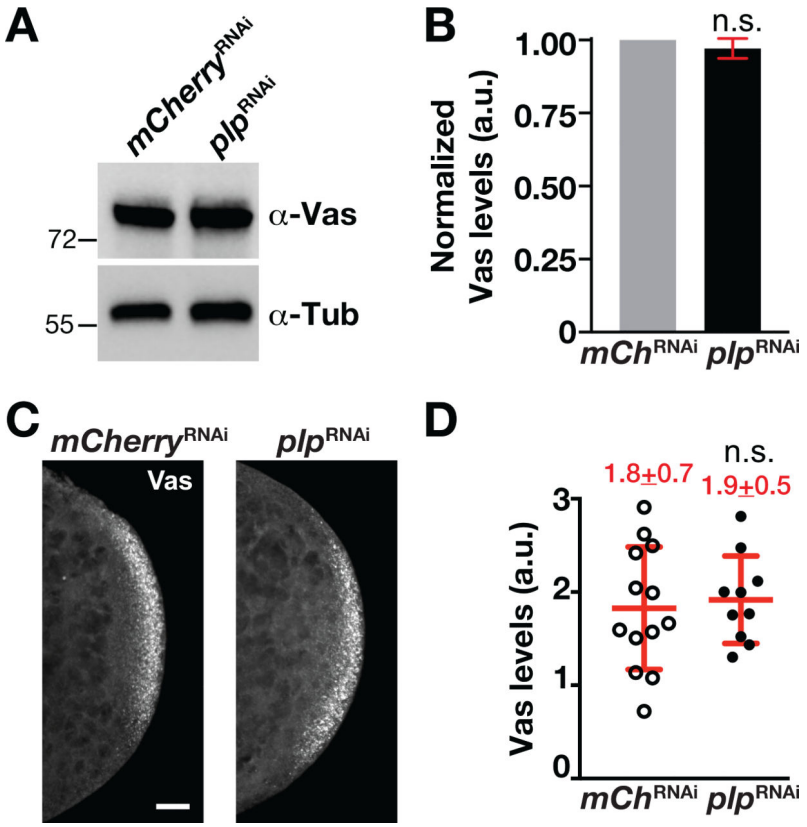

FIGURE 2.

PLP is dispensable for Vas localization to posterior cortex. (a) Western blot analysis of Vas expression from 0–1.5 hr *mCh*^{RNAi} (*mCherry*^{RNAi}) and *plp*^{RNAi} embryo extracts. Anti-α-Tub antibodies were used for normalization. (b) Densitometry quantification of Vas levels from western blot analysis. Vas expression values are relative to the α-Tub loading control and normalized to the *mCherry*^{RNAi}. Error bars show ± *SD* from three replicates. a.u., arbitrary units; n.s., not significant by Student's *t* test. (c). Images show maximum-intensity projections of 0–1.5 hr embryos of the indicated genotypes stained with anti-Vas (gray scale). Bar, 10 μm. (d) Quantification of Vas levels measured within a region-of-interest at the posterior pole. Each data point indicates a single measurement from one embryo, *mCherry*^{RNAi} (*N* = 13 embryos) and *plp*^{RNAi} (*N* = 10 embryos). Mean ± *SD* Vas levels are displayed (red). n.s., not significant by Student's *t* test. The experiment was performed twice with similar results. PLP, Pericentrin-like protein

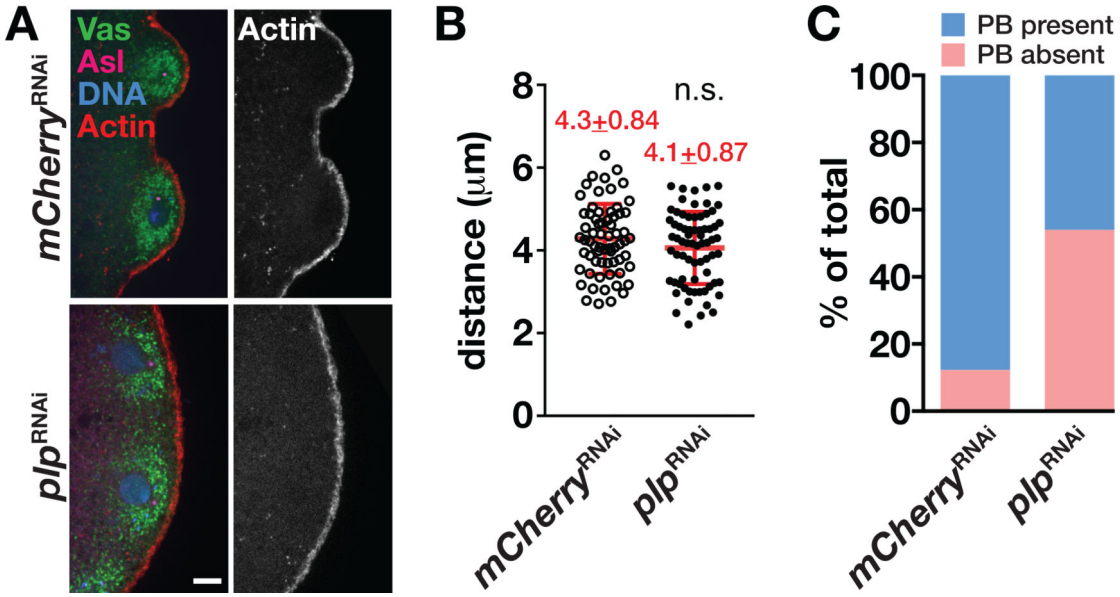

FIGURE 3.

PLP promotes PB protrusion in NC 10 embryos. (a) Single focal plane images of NC 10 embryos of the indicated genotypes stained with anti-Vas (green) to label germ plasm, anti-Asl (magenta) to label the centrioles, and phalloidin (red) to label the actin cortex. Bar, 5 μm. (b) Quantification of the distance between centrosomes and the proximal posterior cortex at NC 10. Each data point indicates the distance between one centrosome and the cortex in $mCherry^{RNAi}$ (N = 66 events in 10 embryos) and plp^{RNAi} (N = 70 events in 12 embryos). Mean ± SD distances are displayed (red). n.s., not significant by Student's t test. The experiment was performed twice with similar results. (c) Quantification of embryos with PB protrusion defects in NC 10. PBs were observed in 88% of $mCherry^{RNAi}$ embryos versus 45% in plp^{RNAi} embryos (N = 33 embryos per genotype). NC, nuclear cycle; PB, pole bud; PLP, Pericentrin-like protein

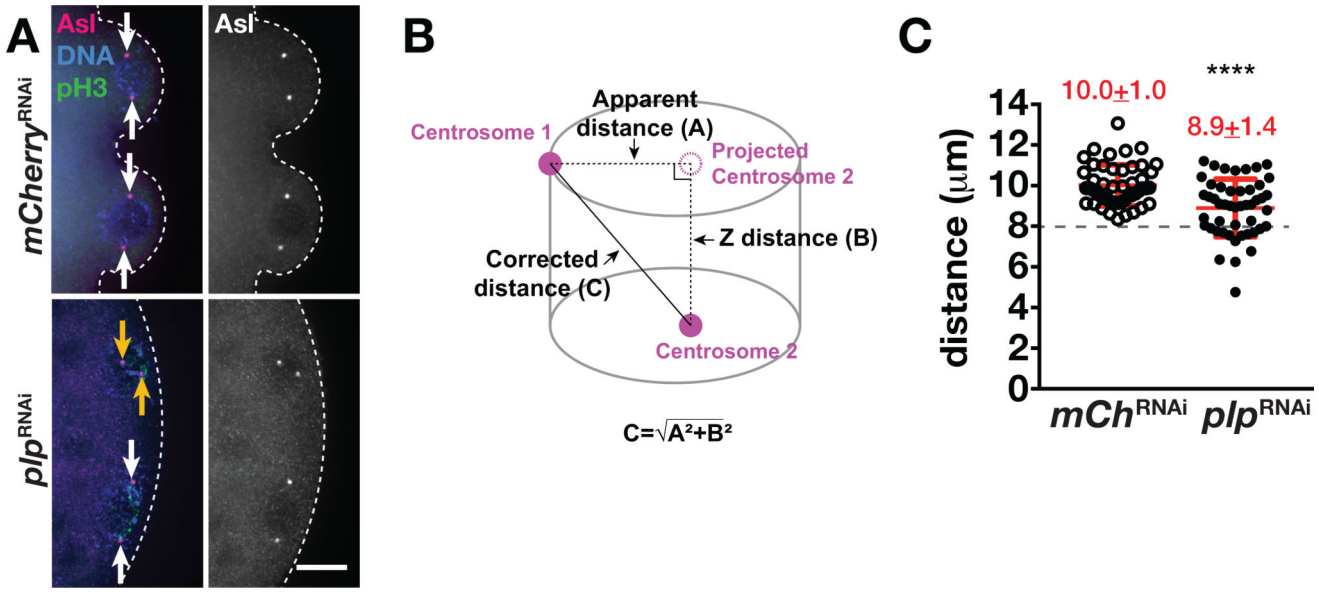

FIGURE 4.

PLP is required for centrosome separation. (a) Images show maximum-intensity projections of prophase-stage NC 10 embryos of the indicated genotypes stained with anti-pH3 (green) to label mitotic nuclei and anti-Asl (magenta) to label the centrosomes. DAPI labels the nuclei (blue). Arrows mark complete (white) or incomplete (orange) centrosome separation. Dashed lines outline the posterior cortex. Bar, 10 μm. (b) Cartoon depicts the distance between a pair of centrosomes. A, represents the apparent distance between centrosomes from a projected image. B, represents the Z-distance between the two centrosomes. C, represents the true distance, as calculated by the Pythagorean theorem. (c) Quantification shows centrosome distance during prophase NC 10 in $mCherry^{RNAi}$ ($N = 49$ events from 12 embryos) and in plp^{RNAi} ($N = 48$ events from 10 embryos). ****$p < .0001$. Mean ± SD are displayed (red). Dashed line indicates 8 μm. The experiment was performed twice with similar results. NC, nuclear cycle; PLP, Pericentrin-like protein

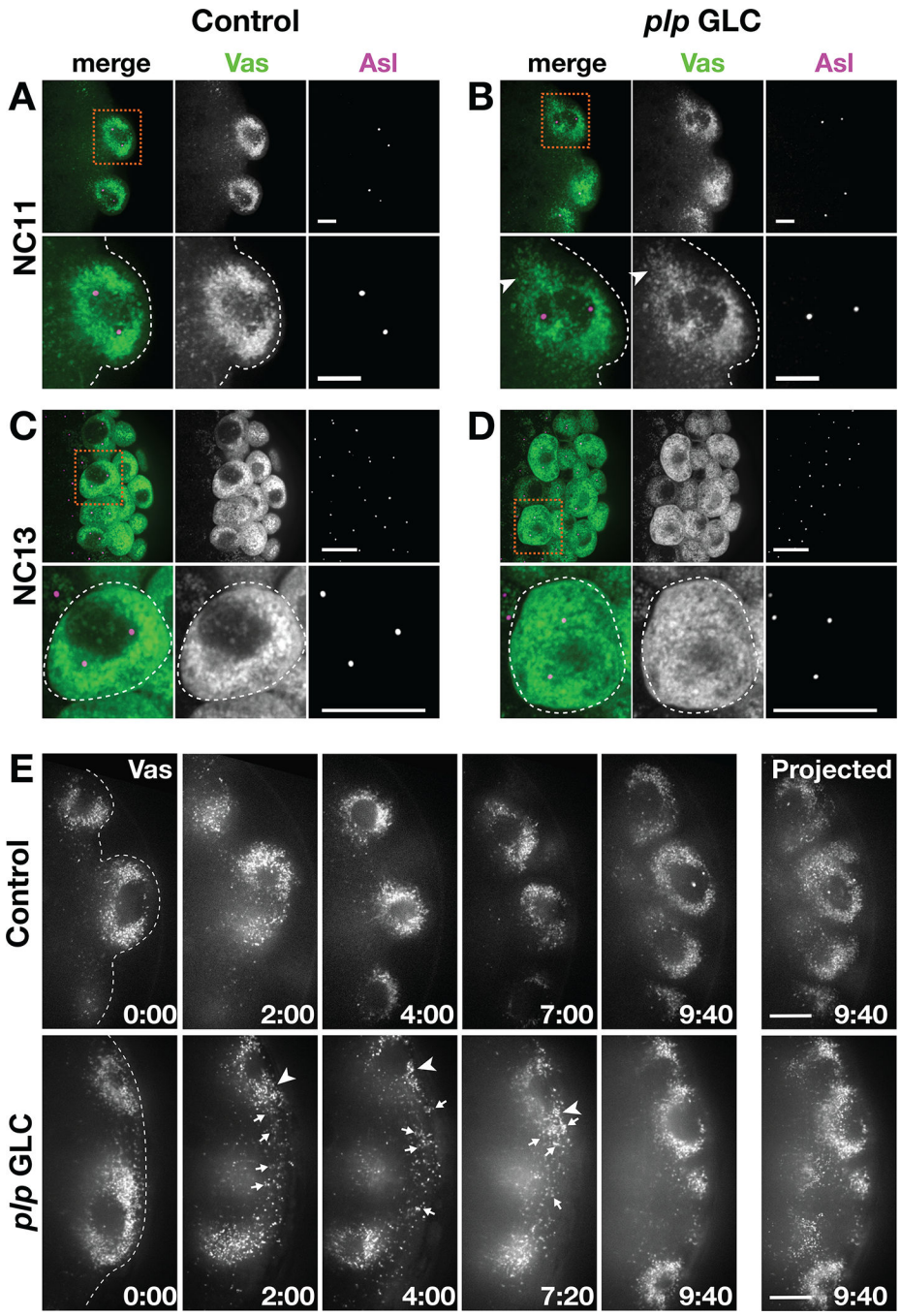

FIGURE 5.

PLP contributes to proper germ plasm distribution. (a–d) Embryos stained with anti-Vas (green) to show the germ plasm, anti-Asl (magenta) labels centrosomes. Boxed region is magnified in inset, below. Dashed line marks the posterior cortex. (a) and (b) Images show maximum-intensity projections of PBs spanning 5 μm of depth in NC 11 embryos. Some *plp* GLC embryos show clusters of Vas that fail to associate with centrosomes (arrowheads). Bar, 5 μm. (c) and (d) Images show maximum-intensity projections of PGCs spanning 0.5 μm of depth in NC 13 embryos. Some *plp* GLC embryos show Vas dispersed in the

cytoplasm of PGCs instead of tightly clustered at the centrosomes. Bar, 10 μm. (e) Stills from time-lapse imaging of GFP-Vas in 1–2 hr control (Video S1) versus *plp* GLC (Video S2) embryos. Images represent a single optical section, and time is shown minutes : seconds. Arrows mark Vas that fails to incorporate into the PB; arrowheads mark Vas less tightly associated with centrosomes. The images on the far right show maximum-intensity projections of PGCs at the end of the movie. Bar, 5 μm. NC, nuclear cycle; PLP, Pericentrin-like protein

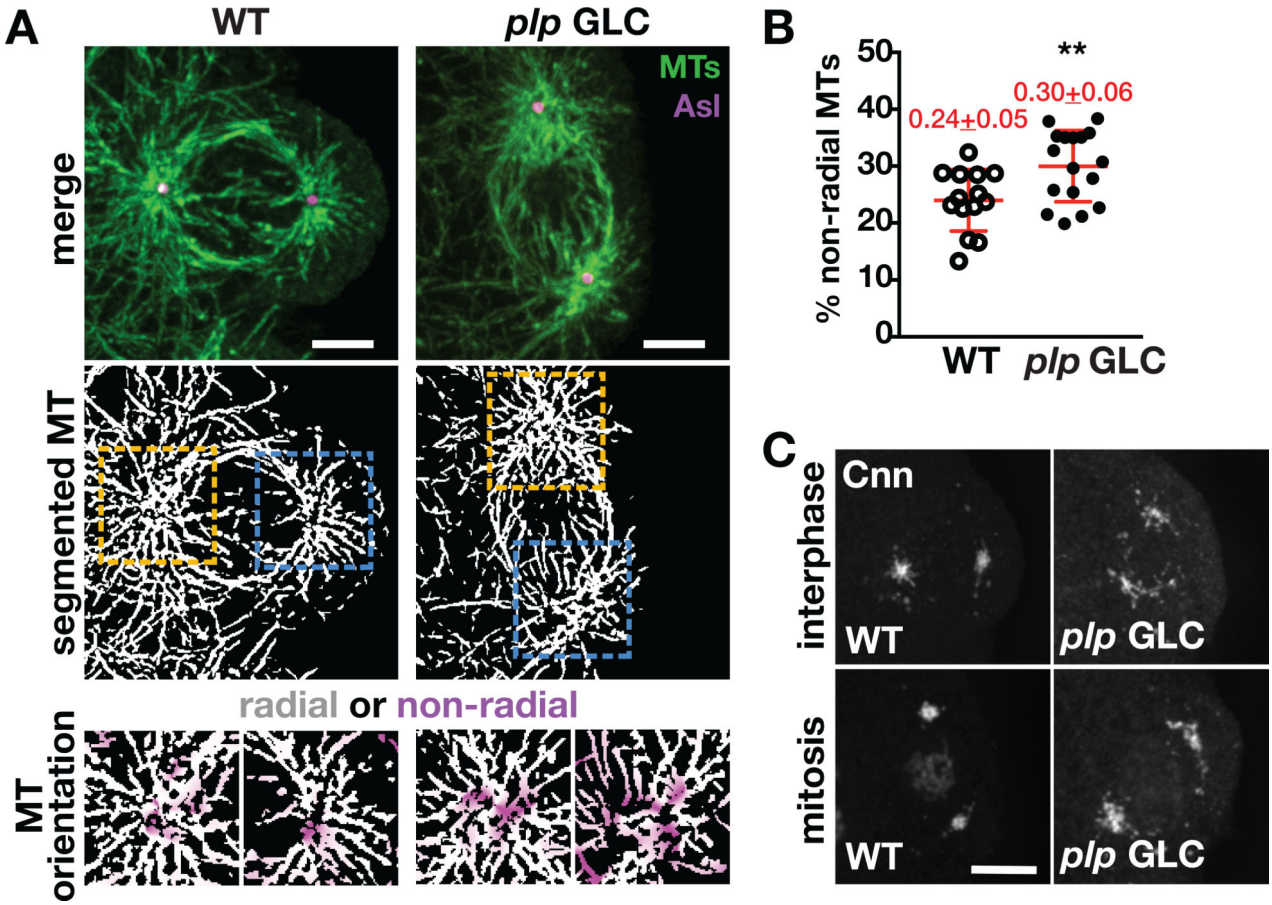

FIGURE 6.

PLP organizes the astral microtubule array within PBs. (a) Microtubule organization in PBs from the indicated genotypes. Top row: single focal plane images stained for α-Tub (MT, green) to visualize microtubule organization in late interphase/early prophase NC 11 embryos costained with anti-Asl (magenta) antibodies. Middle row: segmented images of microtubules. Boxed regions mark region used for radiality analysis, enlarged below. Bottom row: A squared ROI (6 μm dashed square centered on the centriole) was selected and used to measure microtubule radiality. Segmented images were split into a radial and nonradial component based on microtubule orientation relative to the centriole as described in Materials and Methods. Images show merged radial (white) and non-radial (magenta) heat maps. Bar, 5 μm. (b) Quantification of the percentage of nonradial microtubules, as calculated in (a). Each data point represents the ratio of nonradial microtubules at a single centrosome from WT ($N = 14$ events from five embryos) and *plp* GLC ($N = 17$ events from six embryos). Mean ± *SD* are displayed (red). $^{**}p < .01$ by a two-tailed Student's *t* test. (c) Images show maximum-intensity projected PBs in NC 11 embryos of the indicated genotypes stained with anti-Cnn (gray scale). Bar: 5 μm. GLC, germline clone embryo; MT, microtubule; NC, nuclear cycle; PLP, Pericentrin-like protein; WT, wild-type

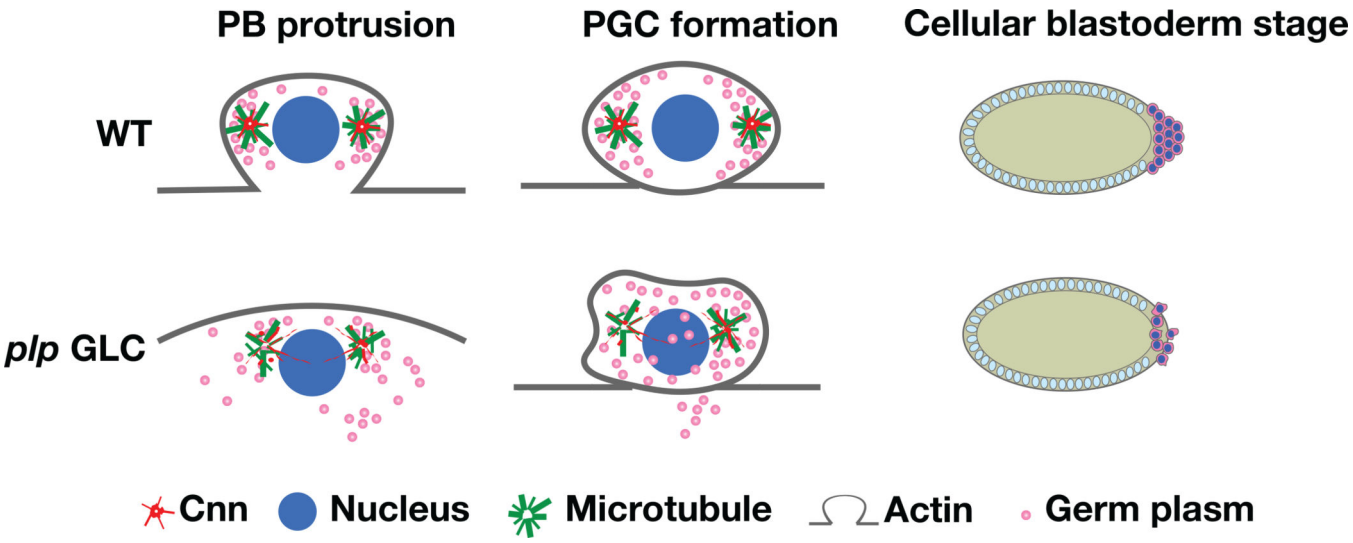

FIGURE 7.

PLP promotes microtubule organization to induce PGC formation. Cartoon model of PLP function during PGC development. The schematic shows normal (WT) PB protrusion during NC 10 requires PLP to promote microtubule organization at the centrosomes, which ensures efficient segregation of the germ plasm into the PGCs. However, loss of *plp* is associated with impaired microtubule organization, resulting in uneven and aberrant germ plasm distributions and a failure to completely partition the germ plasm into the nascent germ cells. Consequently, disruption of PLP abates PGC formation during *Drosophila* embryogenesis. NC, nuclear cycle; PGC, primordial germ cells; PLP, Pericentrin-like protein; WT, wild-type